Science of Sintering, **44** (2012) 65-71

doi: 10.2298/SOS1201065O

UDK 519.718:553.689

Synthesis of Barium-zinc-titanate Ceramics

N. Obradović[1,*], M. V. Nikolić[2], N. Nikolić[2], S. Filipović[1], M. Mitrić[3], V. Pavlović[1], P. M. Nikolić[4], A. R. Đorđević[5], M. M. Ristić[4]

[1] Institute of Technical Sciences of SASA, Knez Mihajlova 35/IV, 11000 Belgrade, Serbia

[2] Institute for Multidisciplinary Research, University of Belgrade, Kneza Višeslava 1a, 11000 Belgrade, Serbia

[3] Institute of Nuclear Sciences Vinča, University of Belgrade Mike Alasa 12-14, 11000 Belgrade, Serbia

[4] Serbian Academy of Sciences and Arts, Knez Mihajlova 35, 11000 Belgrade, Serbia

[5] School of Electrical Engineering, University of Belgrade, Bulevar kralja Aleksandra 73, 11000 Belgrade, Serbia

Abstract:

Mixtures of $BaCO_3$, ZnO and TiO_2 powders, with molar ratio of 1:2:4, were mechanically activated for 20, 40 and minutes in a planetary ball mill. The resulting powders were compacted into pellets and isothermally sintered at 1250 °C for 2h with a heating rate of 10 °C/min. X-ray diffraction analysis of obtained powders and sintered samples was performed in order to investigate changes of the phase composition. The microstructure of sintered samples was examined by scanning electron microscopy. The photoacoustic phase and amplitude spectra of sintered samples were measured as a function of the laser beam modulating frequency using a transmission detection configuration. Fitting of experimental data enabled determination of photoacoustic properties including thermal diffusivity. Based on the results obtained correlation between thermal diffusivity and experimental conditions, as well the samples microstructure characteristics, was discussed.

Keywords: *Ceramics; Mechanochemical processing; Sintering; X-ray diffraction.*

1. Introduction

The phase diagram of the BaO-TiO_2 system determined by Negas et al. [1] has provided key data for understanding and processing barium-titanate dielectric ceramics important for wireless communication technology. Many microwave materials used nowadays are titanate based ceramics [2]. Various ternary systems involving BaO and TiO_2 have been studied due to their specific microwave properties and application in the MW region as parts of resonators, filters and Multilayer Ceramic Capacitors [3].

An extensive discussion of the fundamental crystal chemistry and crystal structures of various polytitanates (such as BaO-TiO_2-ZrO_2, BaO-TiO_2-Al_2O_3, BaO- TiO_2-MgO, BaO-TiO_2-Nb_2O_5, BaO-TiO_2-ZnO) has been reported by Roth et al. [4]. He suggested the phase diagram of the ternary system BaO-TiO_2-ZnO and reported the chemical composition of the

*) **Corresponding author**: obradovic.nina@yahoo.com

compound $BaZn_2Ti_4O_{11}$, with the ratio of the starting oxides being close to 1:2:4. The system contains at least four ternary phases: $Ba_xZn_xTi_{8-x}O_{16}$ with a Hollandite structure, $Ba_4ZnTi_{11}O_{27}$, $Ba_2ZnTi_5O_{13}$ and $BaZn_2Ti_4O_{11}$. The overall structure of $BaZn_2Ti_4O_{11}$ (Orthorhombic *Pbcn*, a=14.140(3)Å, b=11.592(2)Å and c=11.1173(13)Å) consists of a three-dimensional network of distorted, edge-sharing and corner-sharing octahedra with Zn filling some tetrahedral interstices. Ti atoms were found to occupy only octahedral positions [5]. Zn atoms were also found to occupy both tetrahedral and octahedral sites.

It is well known that dielectric properties strongly depend on the synthesis method and conditions such as choice of starting materials, their pre-sintering preparation, sintering temperatures and times, etc [6]. These conditions influence the physical and chemical properties of a material such as particle size, lattice parameter, stoichiometry. From the well-established relationships between these factors and electric properties, therefore, the key point is how to manufacture pure $BaZn_2Ti_4O_{11}$ compound by an easy and low-cost method. From this point of view, mechanochemistry is one of the most promising low temperature methods of synthesis [7]. In this method nanoscale mixing of reagents occurs. The nucleation process is initiated at room temperature, exhibiting a more homogeneous distribution, larger specific surface area and smaller particle size of products as compared with those prepared by the conventional solid state method.

In the present work, we investigated the influence of mechanical activation (MA), combined with subsequent thermal treatment on the crystal structure, microstructure and dielectric properties of $BaZn_2Ti_4O_{11}$ samples.

2. Experimental procedure

MA was carried out in planetary ball mill (Retsch type PH 100), using ZrO_2 jars and balls (10 mm diameter, 400 rpm). The mass ratio of materials to ball was 1/20. $BaCO_3$ (99% Sigma-Aldrich), ZnO (99% Sigma-Aldrich) and TiO_2 (99.8% Sigma-Aldrich) powders were used as starting reagents. The aimed molar ratio was $BaCO_3/ZnO/TiO_2$=1/2/4. Activation was performed for 20, 40 and 80 min. Samples were denoted as BZT-0 to BZT-80, according to the milling time. MA was followed by thermal treatment of the powder mixtures in a tube furnace (Lenton Thermal Design Type 1600) at 1250 ^oC for 2h. The density of specimens was calculated from measurements of the specimen's diameter, thickness and mass.

Phase analysis was performed from the powder diffraction patterns using Philips a PW-1050 automated diffractometer with a Cu tube. Diffraction data were collected in a range 2θ of 10 – 120º counting time 15s and step of 0.02^o.

The morphology of sintered samples was characterized by scanning electron microscopy (JEOL JSM-6390 LV). Dielectric properties were evaluated from capacitance measurements of sintered samples coated with silver electrodes. The capacitances were measured using a network analyzer (Agilent E5062A) in the range 300MHz-2GHz.

Photoacoustic (PA) amplitude and phase spectra of all prepared samples were measured using a PA cell with a transmission detection configuration described in detail in [8]. An 80 mW red laser was used as an optical source and a laser beam was modulated with a mechanical chopper so that the sample was irradiated by a spot about 3 mm in diameter. The samples had a disc shape with the diameter of about 10 mm. When the amplitude and phase diagrams were measured, the sample thickness was decreased. Then the same measurements (PA) were repeated. This was necessary because there is a decrease in the microphone sensitivity in the frequency range lower than 100 Hz. The experimentally PA signals were corrected in the range of low frequency using two different thicknesses of the sample. The normalized amplitude and phase spectra are described with the following equation:

$$\frac{S_1}{S_2} = A_n \exp(j\rho_n) \quad (1)$$

where S_1 and S_2 are the PA signals for two different thicknesses of the same sample. A_n is the amplitude ratio, ρ_n is the phase difference of those two PA signals.

3. Results and Discussion

XRD analysis of BZT 0-80 samples showed that $BaZn_2Ti_4O_{11}$ was obtained in samples with activation times of 0, 20 and 40, while 80 minutes of mechanical activation proved too long as the structure was changed. The initial ratio $BaO/ZnO/TiO_2$ of 0.8:2.07:4.13 slightly departs from the desired 1:2:4 and it is in the stability field of BZT and Zn_2TiO_4. This is further confirmed by XRD analyses of the sintered samples which show the presence of the phase corresponding to $BaZn_2Ti_4O_{11}$ as well as the minor/subordinate spinel phase. The full profile matching refinement (*Le Bail* pattern decomposition) [9] implemented in FullProf software [10] was employed in order to calculate the unit cell parameters of individual phases. The measured XRPD patterns of non-activated samples and samples activated for 20 and 40 minutes are presented in Fig. 1**.**

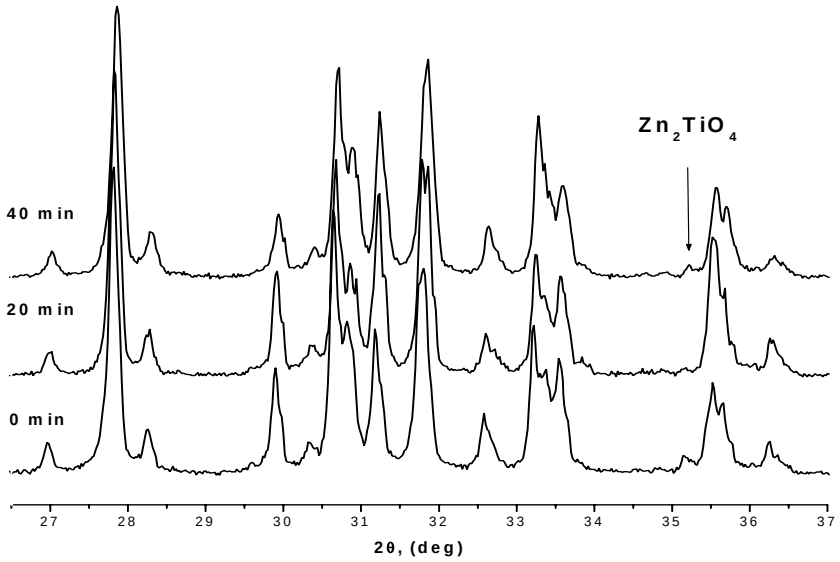

Fig. 1. Region of interest showing reflections of BZT and (311) reflection of Zn_2TiO_4 for a non-activated sample and samples activated for 20 and for 40 min.

Unit cell parameters were calculated using the initial values of unit-cell parameters for $BaZn_{2.03}Ti_{3.93}O_{10.89}$ and Zn_2TiO_4 (ICSD file cards 73841 and 80850, respectively). The calculated values for both phases are given in Tab. I.

The lattice parameters obtained for the major BZT phase show a slight difference (Tab. I) but with no observed trend of their change with activation time. In addition, they are also slightly greater then those reported by Belous et al. [5]. The lattice parameter obtained for the subordinate spinel phase Zn_2TiO_4 showed no change with increased activation time.

Tab I Unit cell parameters for the two-phase BZT system (non-activated (0 min.), activated for 20 and for 40 min.) and Zn_2TiO_4 (note: n.c. – not calculated; uncertainties are 1σ).

BZT	***BZT-0 (0 min)***	***BZT-20 (20 min)***	***BZT-40 (40 min)***
a [Å]	14.14300(19)	14.14559(15)	14.14167(22)
b [Å]	11.60216(17)	11.60202(12)	11.60293(17)
c [Å]	10.12553(13)	10.12635(12)	10.12488(14)
Zn_2TiO_4			
a [Å]	8.4598(14)	n.c.	8.45881(40)

Micrographs of BZT sintered samples are given in Fig. 2. The microstructure of non activated sintered samples is characteristic for early stages of the sintering process and can be described by a non-uniform grain size and a high level of open porosity. Since MA leads to increase in surface activity and mass mobility through the grain boundaries, the microstructure of activated samples is characterized by grain conglomeration and their strengthening. The micrograph of a sample activated for 20 min showed a decrease in the number of pores and their size although grains have retained their structure due to agglomerates within the activated powder. Sintering within agglomerates increased mass transport which resulted in compacted parts of samples and pore spheroidization. Intensive grain growth caused by high activity of the starting powder is specially noticed for the sample activated 40 min.

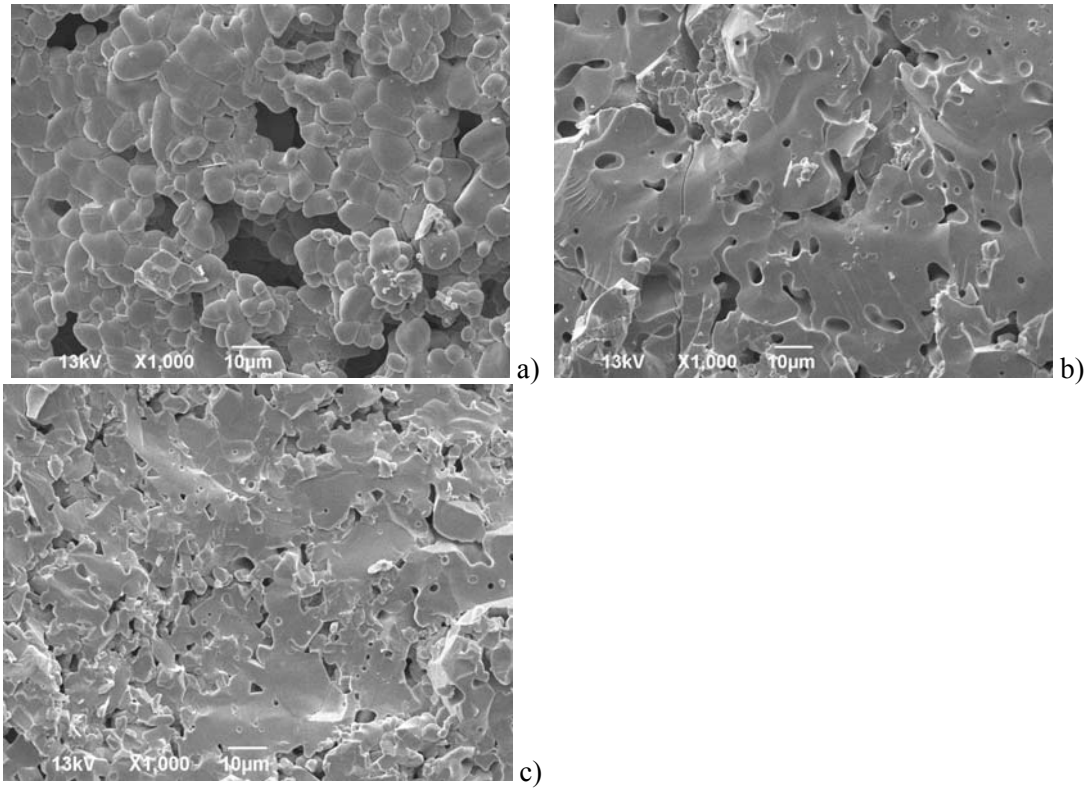

Fig. 2. Scanning electron micrographs of a) BZT-0, b) BZT-20 and c) BZT-40 sintered at 1250 °C for 2h.

Polygonal grains approx. 12 micrometers in size are dominant compared to grains 2-3 micrometers in size that are present in samples activated for lower milling times. The process of grains coalescence is complete, pores are closed and spherical and the final sintering stage leads to predicted densification.

The results of microstructure development are in accordance with dielectric properties of the samples. The values of density changes during the sintering process (*ds*, ρ given in % of the theoretical density of $BaZn_2Ti_4O_{11}$, ρ_T=5.067 gcm^{-3}), and relative dielectric permittivity (ε_r) of samples sintered at 1250 °C for 2h are given in Tab II.

Tab. II Relative shrinkage and dielectric properties of samples non-activated and activated 20 and 40 min and sintered at 1250 °C for 2h in the microwave region.

sample	***ds (%TD)***	ε_r
BZT-0	62.42	11.40
BZT-20	81.55	20.20
BZT-40	87.49	20.70

The electrical measurements pointed out that the dielectric permittivity of the specimens increased with activation time, reaching its maximum value for the sample activated for 40 minutes. According to our analysis, since a higher density resulted in a higher dielectric permittivity owing to a lower porosity for the fixed sintering temperature, and since we obtained almost pure $BaZn_2Ti_4O_{11}$ phase, as observed from XRD patterns, the changes in dielectric permittivity are caused only by the densification effect. This suggest that, for the activation and sintering conditions we used, a higher density and the homogeneity of morphology are dominantly responsible for the higher values of dielectric permittivity of the samples.

In this work we have used an efficient method for the normalization of the photoacoustic signals. The signal ratio for two different thicknesses of each measured sample was calculated using the equation (1). For each non-activated sample and samples activated for 20 and 40 min we have made normalized PA amplitude and phase spectra for two various thicknesses. A typical example of a fitted phase diagram is given in Fig. 3.

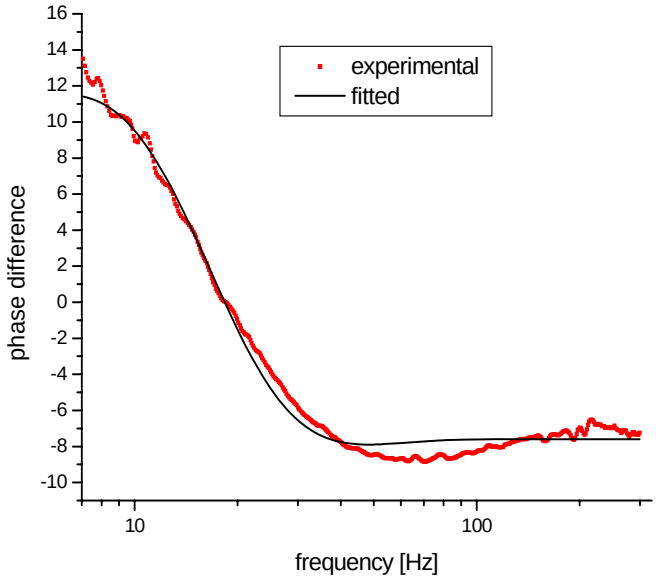

Fig. 3. Phase difference for normalized PA phase spectra measured for two different thicknesses for a non-activated sample.

The experimental curves were compared with theoretical ones using the mathematical model given in Ref. [8]. Values of the following fitted parameters: D_T - the thermal diffusivity coefficient; α - the optical absorption coefficient, τ - the excess carrier lifetime; D – carriers diffusion coefficient; s_g – first surface recombination velocity; Eg – the energy gap and also K – the thermal conductivity are given in Tab. III. With the activation procedure the thermal diffusivity coefficient increased but the absorption coefficient, carrier diffusion coefficient and s_g decreased.

Tab. III Values of fitted parameters.

sample	D_T (m^2/s)	α (m^{-1})	τ (s)	D (m^2/s)	s_g (m/s)	*Eg (eV)*	*K (W/mK)*
BZT0	$0.14\cdot10^{-6}$	1491	$0.47\cdot10^{-1}$	$0.60\cdot10^{-5}$	254	2.91	1.8
BZT20	$0.47\cdot10^{-5}$	1316	$0.31\cdot10^{-2}$	$0.128\cdot10^{-6}$	1.6	2.84	1.37
BZT40	$0.57\cdot10^{-5}$	742	$0.17\cdot10^{-2}$	$0.44\cdot10^{-7}$	0.9	2.87	1.48

4. Conclusions

In this paper synthesis of barium-zinc-titanate was analyzed. Mixtures of $BaCO_3$, ZnO and TiO_2 were mechanically activated for 20, 40 and 80 minutes in a planetary ball mill and then isothermally sintered at 1250 ^oC for 2h. X-ray diffraction analyses confirmed the formation of barium-zinc-titanate in along with a slight amount of spinel zinc-titanate phase in samples activated for 0, 20 and 40 minutes. The photoacoustic phase and amplitude diagrams of sintered barium-zinc-titanate samples were measured in relation to the frequency of the chopped laser beam. It was shown that thermal diffusivity and also dielectric permittivity of this material increased with the activation time in accordance with changes in the densities of sintered samples.

Acknowledgement

This research was performed within projects 172057, III45007 financed by the Ministry for Science and Education of the Republic of Serbia and project F-198 financed by Serbian Academy of Science and Arts.

5. References

1. T. Negas, R.S. Roth, H.S. Parker, D. Minor, J. Solid State Chem. 9 (1974) 297.
2. W. Wong-Ng, R.S. Roth, T.A. Vanderah, H.F. McMurdie, J. Res. Natl. Inst. Stand. Technol. 106 (2001) 1097.
3. 3 W. Guoquing, W. Shunhua, Mater. Lett. 59 (2005) 2229.
4. R.S. Roth, C.J. Rawn, C.G. Lindsay, W. Wong-Ng, J. Solid State Chem. 104 (1993) 99.
5. A.G. Belous, O.V. Ovchar, M. Macek-Krzmanc, M. Valant, J. Eur. Ceram. Soc. 26 (2006) 3733.
6. A.S. Khim, J. Wang, X. Junmin, J. of Alloys and Comp. 311 (2000) 181.
7. N. Obradović, S. Filipović, V. B. Pavlović, A. Maričić, N. Mitrović, I. Balać, M. M. Ristić, Sci. Sint. 43 (2011) 145.
8. P.M. Nikolic, D.M. Todorovic, S.S. Vujatovic, S. Djuric, P. Mihajlovic, V. Blagojevic, K.T. Radulovic, A.I. Bojicic, D. Vasiljevic-Radovic, J. Elazar, D. Urosevic, Jpn. J. Appl. Phys. 37 (1998) 4925.
9. A. Le Bail, H. Duroy & J.L. Fourquet, Mat. Res. Bull. 23 (1988) 447.

10. J. Rodriguez-Carvajal, Physica B. 192 (1993) 55.

Садржај: *Смеше прахова $BaCO_3$, ZnO и TiO_2 у моларном односу 1:2:4, механички су активирани 20, 40 и 80 минута у планетарном млину. Тако добијени прахови су компактирани у таблете и синтеровани изотермски на 1250 °C 2 сата са брзином загревања од 10 °C/min. Рендгенска дифракциона анализа добијених прахова и синтерованих узорака урађена је да би се испитале структурне промене у фазном саставу. Скенирајућом електронском микроскопијом испитивана је микроструктура синтерованих узорака. Фотоакустични спектри фазе и амплитуде синтерованих узорака мерени су као функција фреквенције ласерског спектра помоћу трансмисионог конфигурационог детектора. Фитовање експерименталних података омогућило је одређивање фотоакустичних својстава укључујући и термалну дифузивност. На основу добијених резултата, продискутовани су однос између термалне дифузивности и експерименталних података као и микроструктурне карактеристике синтерованих узорака.*

Кључне речи: *керамика; механохемијско процесирање; синтеровање; рендгенска дифракција.*